

# PHYSICAL REVIEW E

## STATISTICAL PHYSICS, PLASMAS, FLUIDS, AND RELATED INTERDISCIPLINARY TOPICS

THIRD SERIES, VOLUME 57, NUMBER 1

JANUARY 1998

### RAPID COMMUNICATIONS

*The Rapid Communications section is intended for the accelerated publication of important new results. Since manuscripts submitted to this section are given priority treatment both in the editorial office and in production, authors should explain in their submittal letter why the work justifies this special handling. A Rapid Communication should be no longer than 4 printed pages and must be accompanied by an abstract. Page proofs are sent to authors.*

#### Thermodynamic approach to electrical tree formation

J. L. Vicente,<sup>1</sup> A. C. Razzitte,<sup>2</sup> M. C. Cordero,<sup>1</sup> and E. E. Mola<sup>1,\*</sup>

<sup>1</sup>INIFTA, División Química Teórica, Sucursal 4, Casilla de Correo 16, La Plata 1900, Argentina

<sup>2</sup>LAFMACEL, Departamento de Química, Facultad de Ingeniería, Universidad de Buenos Aires, Buenos Aires, Argentina

(Received 4 June 1997)

A statistical picture of dielectric breakdown in solids for a linear two-dimensional geometry is presented and discussed in this paper. The difference between branched structures grown on an open-planar geometry, such as those studied by Sato and Hayakawa [Phys. Rev. Lett. **79**, 95 (1997)] or by Elezgaray *et al.* [Phys. Rev. Lett. **71**, 2425 (1993)], and those structures grown on a linear two-dimensional geometry, like the one used in the present paper to model dielectric breakdown, is not trivial and should be demonstrated. Boundary conditions of an open-planar geometry are placed at infinity and therefore the morphology selection mechanism can be studied by diffusion-limited aggregation (DLA) in two dimensions, as was done by Sato and Hayakawa. Unfortunately, the DLA approach cannot be used to model dielectric breakdown on a linear two-dimensional geometry. This paper shows that the underlying morphology selection process does not depend strongly upon the geometry. [S1063-651X(98)50301-7]

PACS number(s): 05.70.Ln, 02.50.-r

In the past few years, considerable theoretical and experimental efforts have been undertaken to investigate the scaling properties of rough surfaces of compact clusters. In the past couple of decades, diffusion-limited aggregation (DLA) has been recognized as one of the most plausible models for many varieties of nonequilibrium growth phenomena including dielectric breakdown, fingering of viscous fluids, surface roughness, electrochemical deposition, and so on. In studies of irreversible growth, one of the most essential and remaining problems is the morphology selection mechanism during stochastic growth processes. How probable is the form we observe in computer simulations or experiments? What about the fluctuation of morphology during growth? To answer these questions, one has to consider the ensemble of total growth histories as a snapshot, rather than observed clusters, which is the subject of statistical mechanics.

Recently, Sato and Hayakawa [1] have introduced a formalism of irreversible aggregation processes in terms of statistical mechanics. Thermodynamical variables that include

the degeneracy of the histories, which they call “history entropy,” are introduced by taking into account all possible growth histories. By considering the thermodynamic properties of the growth history and harmonic measure, they found the condition of the most probable history for diffusion-limited aggregation (DLA) as a function of the mass fractal dimension of the resulting clusters. The “history entropy” concept was previously introduced by Elezgaray *et al.* [2] under the name of “history probability,” that is, the probability of finding a history from a seed particle to a resultant cluster, and they studied the morphology selection mechanism of Laplacian growth.

The difference between branched structures grown on an open-planar geometry, such as those studied by Sato and Hayakawa [1] or by Elezgaray *et al.* and those structures grown on a linear two-dimensional geometry, like the one used in the present paper to model dielectric breakdown, is not trivial and should be demonstrated. Boundary conditions of an open-planar geometry are placed at infinity and therefore, the morphology selection mechanism can be studied by diffusion-limited aggregation (DLA) in two dimensions, as was done by Sato and Hayakawa. Unfortunately, the DLA

\*Author to whom correspondence should be addressed.

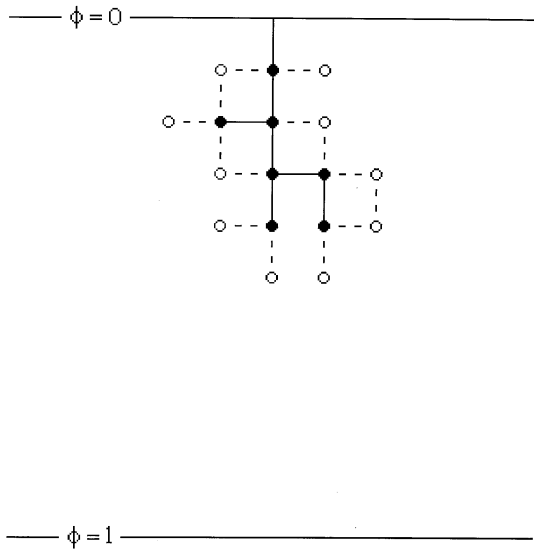


FIG. 1. Illustration of the two-dimensional model for simulating the dielectric breakdown model. The upper horizontal line represents the electrode and the perpendicular segment represents the tip where the discharge simulation begins. The other electrode is modeled by the lower horizontal line. The discharge pattern is indicated by the black dots connected by thick lines and it is considered equipotential ( $\phi=0$ ). The dashed bonds indicate all of the possible growth processes. The probability for each of these processes is proportional to the local electric field.

approach cannot be used to model dielectric breakdown [3].

This paper shows how the statistical-mechanics methods can be applied to describe the distribution of electrical trees generated in a growth model on a linear two-dimensional geometry.

A two-dimensional square lattice (Fig. 1), in which two opposite sides represent the two electrodes, is considered. Breakdown starts at a point of a high local field and this enhancement is usually attributed to electrically conducting inclusions. The conducting inclusions are represented by electrode pins. Discharge simulation begins at one of the electrode pins where a short filament represents the tip of one pin. The rules assumed for the growth of the discharge pattern (the electrical tree) are as follows.

(1) The electrical tree grows stepwise. The discharge structure has zero internal resistance, i.e., at each point of the structure the electric potential  $\phi$  is  $\phi=0$ , whereas at the counterelectrode it is  $\phi=1$ . The discrete form of Laplace equation

$$\phi_{i,k} = \frac{1}{4}(\phi_{i+1,k} + \phi_{i-1,k} + \phi_{i,k-1} + \phi_{i,k+1}) \quad (1)$$

is solved with the previous boundary conditions.

(2) The probability that a bond will form between a point that is already part of the electrical tree and a new adjacent point is a function of the local field between the two points (i.e., the potential difference between the two points). A power-law dependence with exponent  $\eta$  is assumed and the probability associated with points  $i,k$  at the structure and  $i',k'$  adjacent to but outside it is given by

$$P(i,k \rightarrow i',k') = \frac{(\phi_{i',k'})^\eta}{\sum_{(j,l) \in \Gamma} (\phi_{j,l})^\eta} \quad (2)$$

The sum in the denominator refers to all of the possible

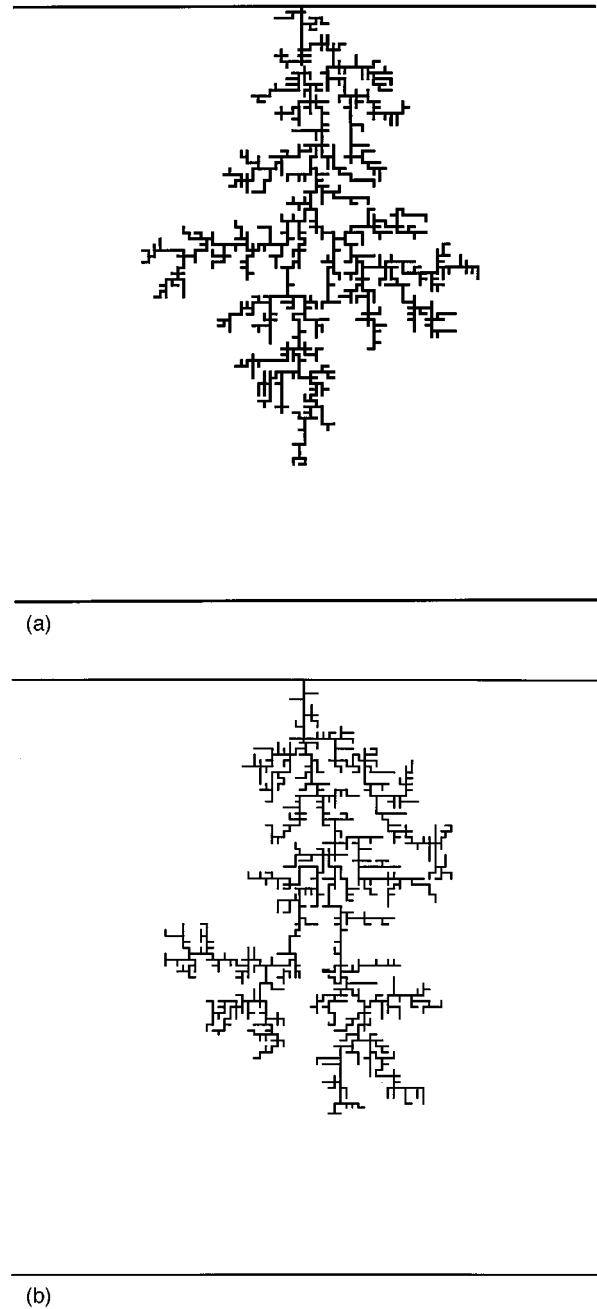


FIG. 2. Two simulated tree patterns obtained with the model, with the same field exponent  $\eta$  ( $\eta=1$ ); (a) a characteristic history pattern, (b) a pattern with a higher probability history.

growth sites  $(j,l)$  adjacent to the electrical tree, where  $\Gamma$  is the set of possible candidates to be incorporated into the electrical tree.

(3) A new bond (and point) is chosen randomly and added to the electrical tree.

(4) With the new electrical tree and the new boundary conditions the process starts again. A couple of tree patterns obtained from the model are shown in Fig. 2 for a constant  $\eta$  value ( $\eta=1$ ).

According to the growth rule of the  $\eta$  model, a collection of electrical trees  $C_M$  of “mass  $M$ ” (number of bonds) is obtained and the branching structures  $C_M$  give the state of damage as a function of “time” (number of bonds). In this context, a probability  $p(C_M, \eta)$  for each  $C_M$  can be assigned to each value of  $\eta$ .

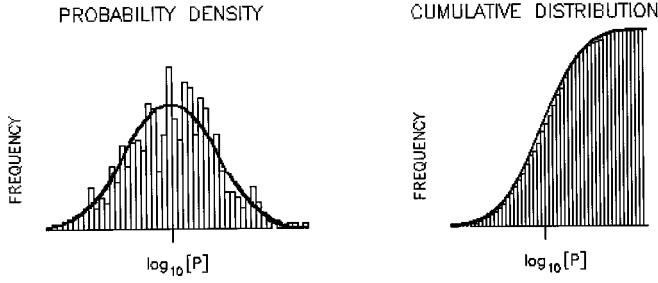


FIG. 3. Histogram of the probability distribution of the  $p(C_M, \eta)$  values, with  $M$  and  $\eta$  fixed ( $\eta=0.5$  and  $M=300$ ). The histogram is adjusted by means of a normal distribution.

Based on a number of numerical simulations, an expression equivalent to that employed for open-planar geometry by Elezgaray *et al.* [2] is obtained as

$$\ln[p(C_M, \eta)] = S(C_M) + A(C_M)\beta(\eta) + \alpha(\eta, M), \quad (3)$$

where  $\beta(\eta)$  and  $\alpha(\eta, M)$  are two universal functions,  $A(C_M)$  plays the role of the energy of the electrical tree, and  $S(C_M)$  is a history degeneracy factor. The above expression for  $p(C_M, \eta)$  has the form of a Boltzmann weight if  $\beta(\eta)$  is identified with the inverse of the temperature and  $\alpha(\eta, M)$  with the free energy. Then, the following equation can be written as

$$\alpha(\eta, M) = -\ln \left\{ \sum_{|C_M|=M} \exp[S(C_M) + A(C_M)\beta(\eta)] \right\}. \quad (4)$$

This paper is mainly devoted to providing evidence for Eq. (3) in the above-mentioned electrode geometry.

If Elezgaray's notations are adopted, a history  $h$  is a sequence  $\{s_1, s_2, \dots, s_M\}$  of  $M$  sites in the interelectrode gap (included in  $Z \times Z$ ), so that for each  $m \leq M$ ,  $s_m = (i_m, k_m)$  is the node incorporated into the electrical tree at the step  $m$ .  $H(C_M)$  is the set of various possible histories that lead to the electrical tree  $C_M$ .

For each value of  $\eta$ , the probability of any history  $h$  is defined by

$$P(h, \eta) = \prod_{m=1}^M \frac{\phi_{i_m, k_m}^\eta}{\sum_{(i', k') \in \Gamma_n(h)} \phi_{i', k'}^\eta}, \quad (5)$$

where for each  $m \leq M$  the potential distribution  $\phi_{i, k}$  on the  $m$ th outer boundary  $\Gamma_m(h) = \Gamma\{s_1, s_2, \dots, s_m\}$  is determined. Moreover,  $p(C_M, \eta)$  is normalized over the set of all the electrical trees of mass  $M$ :

$$\sum_{|C_M|=M} p(C_M, \eta) = 1. \quad (6)$$

Any history that maximizes the distribution of history probabilities  $P(p)$  is called a "characteristic history" of the electrical tree  $C_M$  for a given  $\eta$ . The  $M=1000$  tree pattern shown in Fig. 2(a) belongs to the set of characteristic history patterns. These characteristic histories are different from those occurring with the highest probabilities [4]. An  $M=1000$  tree pattern with a higher probability history is shown in Fig. 2(b). A characteristic history pattern is gener-

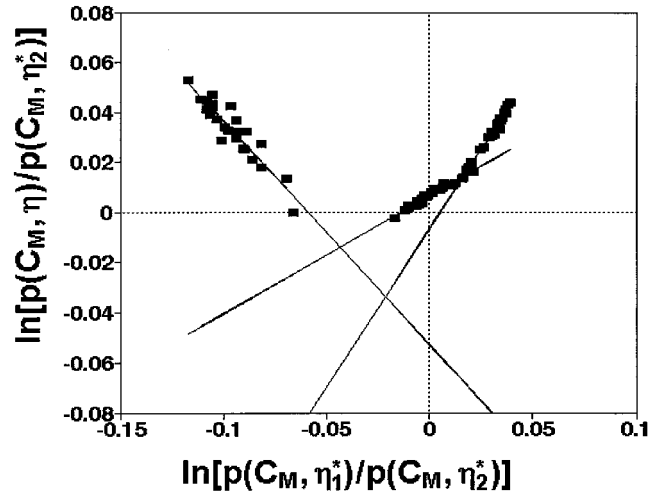


FIG. 4.  $\ln[p(C_M, \eta)/p(C_M, \eta_1^*)]$  vs  $\ln[p(C_M, \eta_1^*)/p(C_M, \eta_2^*)]$ , as computed for a representative statistical sample of  $\eta$  branched structures of mass  $M=100$ . Data come from the saddle-point approximation. The straight lines are linear regression fits for the evaluation of  $b(\eta, M)$  and  $m(\eta)$ .

ally more "symmetrical" (with respect to an axis containing the tip) than those with a higher probability history.

To begin the study of the distribution of electrical trees, various sets of 500 electrical trees of mass  $M=100, 200, 300, 400, 500, 600, 700, 800, 900$ , and  $1000$ , statistically generated with different values of the growth parameter  $\eta=0.5, 1.0, 1.5, 2.5, 3.0, 3.5, 4.0, 4.5$ , and  $5.0$  are computed.

Figure 3 shows the distribution of probability density histories  $p(C_M, \eta)$  for different values of the field exponent  $\eta$ . The corresponding histogram is adjusted by means of a normal (Gaussian) distribution. The standard deviation ( $\sigma$ ) of the normal distribution increases when the field parameter  $\eta$  is increased.

By using the approximate saddle-point method [2],

$$p(C_M, \eta) \approx \sigma(C_M) p[h_c(C_M), \eta], \quad (7)$$

where  $h_c(C_M)$  is any characteristic history of  $C_M$ .

In Fig. 4,  $\ln[p(C_M, \eta)/p(C_M, \eta_1^*)]$  versus  $\ln[p(C_M, \eta_1^*)/p(C_M, \eta_2^*)]$  was plotted for two different trees

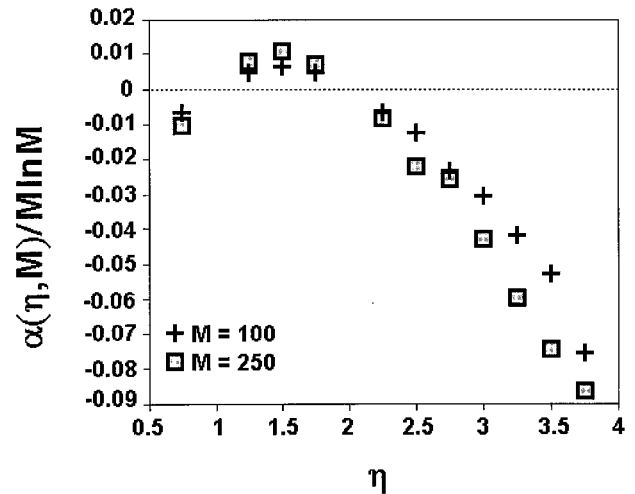


FIG. 5. Estimation of  $m(\eta)$  for  $M=100$  and  $M=250$ .

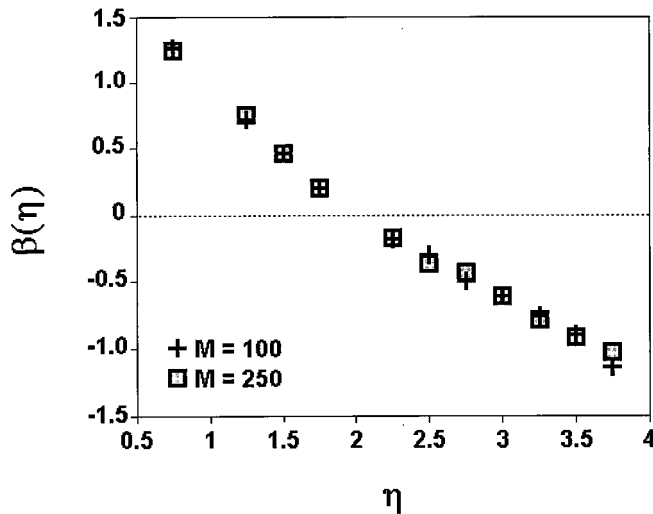


FIG. 6. Estimation of  $b(\eta, M)/M \ln M$  for  $M=100$  and  $M=250$ .

of mass  $M=100$  and  $M=250$ , respectively, for different values of the field exponent  $\eta$  at the interval  $[0,5]$ . Our choice of  $\eta_1^*=1$  and  $\eta_2^*=2$  is arbitrary. The following equation can be written from Fig. 4:

$$\begin{aligned} \ln[p(C_M, \eta)] &= \ln[p(C_M, \eta_2^*)] \\ &+ m(\eta) \ln[p(C_M, \eta_1^*)/p(C_M, \eta_2^*)] \\ &+ b(\eta, M), \end{aligned} \quad (8)$$

where  $m(\eta)$  and  $b(\eta, M)$  (the slope and the value at the origin, respectively) are obtained by linear regression fits and are plotted in Figs. 5 and 6. By comparison with Eqs. (3) and (8),  $b(\eta, M)$  is identified with  $\alpha(\eta, M)$ , and  $m(\eta)$  with  $\beta(\eta)$ , whereas  $\ln[p(C_M, \eta_1^*)/p(C_M, \eta_2^*)]$  is identified with the branching structure energy  $A(C_M)$  and  $\ln[p(C_M, \eta_2^*)]$  with the degeneracy factor  $S(C_M)$ .

In summary, the following conclusions can be drawn: (i)  $\beta(\eta)$  is independent of  $M$ , even for  $M$  as small as  $M=100$ . (ii)  $\alpha(\eta, M)$  scales as  $M \ln M$ . (iii) Our choice for the  $\eta_1^*$ ,  $\eta_2^*$  is arbitrary.

It is clear that  $\beta(\eta)$  and  $\alpha(\eta, M)/M \ln M$ , as well as the degeneracy factor  $S(C_M) \equiv \ln[p(C_M, \eta_2^*)]$ , depend upon this choice, although they only change by additive and multiplicative constants. Both Figs. 5 and 6 clearly show the convergence of  $\beta(\eta)$  and  $\alpha(\eta, M)/M \ln M$  towards two universal, mass-independent functions.

To check the consistency of Eq. (3), let us compute the mean of the branched structure energy  $\langle A \rangle_\eta$  for various sets of 40 branched structures of mass  $M=100$  and 250, statistically generated with different values for the field exponent,  $\eta=0.5, 1, 2, 3, 4$ , and 5:

$$\langle A \rangle_\eta = \langle \ln[p(C_M, \eta_1^*)/p(C_M, \eta_2^*)] \rangle_\eta$$

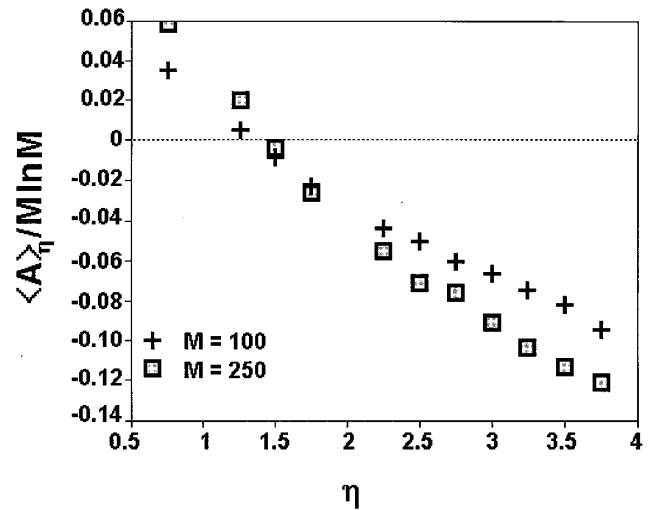


FIG. 7. Mean energy  $\langle A \rangle_\eta$  of the branched structure vs  $\eta$ , as estimated from a sample of 40 branched structures of mass  $M=100$  and 250, statistically generated with different values for the field exponent  $\eta$ .

$$\begin{aligned} &= \sum_{|C_M|=M} p(C_M, \eta) \ln[p(C_M, \eta_1^*)/p(C_M, \eta_2^*)] \\ &= -\alpha'(\eta, M)/\beta'(\eta) = -d\alpha(\eta, M)/d\beta(\eta). \end{aligned} \quad (9)$$

Data plotted in Fig. 7 were obtained from Eq. (4) by plotting  $\alpha(\eta, M)$  as a function of  $\beta(\eta)$  from Figs. 5 and 6. From such a plot the derivative  $-d\alpha/d\beta$  of Eq. (9) was evaluated and plotted in Fig. 7 for two different  $M$  values ( $M=100$  and 250).

Numerical simulations of the  $\eta$  model applied to a two-dimensional stochastic model of electrical treeing in solid dielectrics were carried out. It was found that simulated trees display behavior remarkably similar to that found experimentally. The probability distribution of these branched structures is given by a Boltzmann weight, Eq. (3), where the inverse temperature  $\beta(\eta)$  depends only upon the growth parameter  $\eta$  (see Fig. 5), while the free energy  $\alpha(\eta, M)$  scales as  $M \ln M$  as an extensive thermodynamic quantity. The Boltzmann weight, Eq. (3), also involves a history entropy factor  $S(C_M)$  that is proportional to the logarithm of the total number of histories leading to  $C_M$  [see Eq. (7)]. To the best of our knowledge, this is the first evidence that electrical trees grown on a lattice with axial symmetry exhibit the statistical-mechanics properties reported in this paper.

This research project was financially supported by the Consejo Nacional de Investigaciones Científicas y Técnicas, the Comisión de Investigaciones Científicas de la Provincia de Buenos Aires, and the Universidad Nacional de La Plata. The authors are also indebted to Fundación Antorchas for a grant.

[1] S. Sato and Y. Hayakawa, Phys. Rev. Lett. **79**, 95 (1997).  
 [2] J. Elezgaray, J. F. Muzy, F. Argoul, and A. Arneodo, Phys. Rev. Lett. **71**, 2425 (1993).

[3] E. E. Mola, M. C. Cordero, A. Razzitte, and J. L. Vicente (unpublished).  
 [4] T. Vicsek, F. Family, J. Kerstéz, and D. Platt, Europhys. Lett. **2**, 823 (1989).